

Hepatitis-C-virus-induced microRNAs dampen interferon-mediated antiviral signaling

Abigail Jarret¹, Adelle P McFarland^{1,6,7}, Stacy M Horner^{1,6,7}, Alison Kell¹, Johannes Schwerk¹, MeeAe Hong¹, Samantha Badil¹, Rochelle C Joslyn¹, Darren P Baker^{2,6}, Mary Carrington^{3,4}, Curt H Hagedorn⁵, Michael Gale Jr¹ & Ram Savan¹

Hepatitis C virus (HCV) infects 200 million people globally, and 60–80% of cases persist as a chronic infection that will progress to cirrhosis and liver cancer in 2–10% of patients^{1–3}. We recently demonstrated that HCV induces aberrant expression of two host microRNAs (miRNAs), miR-208b and miR-499a-5p, encoded by myosin genes in infected hepatocytes⁴. These miRNAs, along with AU-rich-element-mediated decay, suppress *IFNL2* and *IFNL3*, members of the type III interferon (IFN) gene family, to support viral persistence. In this study, we show that miR-208b and miR-499a-5p also dampen type I IFN signaling in HCV-infected hepatocytes by directly down-regulating expression of the type I IFN receptor chain, *IFNAR1*. Inhibition of these miRNAs by using miRNA inhibitors during HCV infection increased expression of *IFNAR1*. Additionally, inhibition rescued the antiviral response to exogenous type I IFN, as measured by a marked increase in IFN-stimulated genes and a decrease in HCV load. Treatment of HCV-infected hepatocytes with type I IFN increased expression of myosins over HCV infection alone. Since these miRNAs can suppress type III IFN family members, these data collectively define a novel cross-regulation between type I and III IFNs during HCV infection.

HCV is a single-stranded hepatotropic RNA virus against which no vaccine currently exists. Previously, the standard of care for chronic HCV infection was combination treatment with pegylated IFN- α (pegIFN- α) and ribavirin, which produced a sustained virological response in fewer than 40% of patients⁵. With the addition of protease inhibitors, a type of direct-acting antiviral (DAA), to pegIFN- α and ribavirin therapy, viral cure rates have improved to 56–95% of patients; the exact rate is dependent on both virus and host factors^{6–9}. Following this success, therapeutic advancements have focused on interfering with the viral lifecycle, and many new DAA drugs are

currently in clinical trials^{6,10}. More recently, interferon-free combinations of HCV protease and RNA polymerase inhibitors, sometimes with ribavirin, have produced dramatic results in a subset of patients¹⁰. However, the emergence of resistant HCV variants and the high cost of DAA treatments might limit the availability of these therapies worldwide^{11–13}. The usefulness of DAA-based therapies for some patients—such as those with advanced infection, who are at the highest risk for hepatic decompensation, liver failure, hepatocellular carcinoma and/or death—also remains to be fully proven¹³. Hence, it is critical to identify the mechanisms that HCV employs which lead to the failure of type I IFN therapy. In this study, we show that HCV dampens type I IFN signaling by targeting *IFNAR1* mRNA expression. This novel mechanism not only provides insight into why IFN-based HCV therapies have failed but also suggests why the interferon lambda 3 (*IFNL3*) genotype correlates with the outcome of type I IFN treatment.

Several viral and host factors are predictive of HCV clearance, including viral genotype, baseline viral load and host genotype. Genome-wide association studies have identified three single-nucleotide polymorphisms (SNPs) near the antiviral *IFNL3* gene that associate with natural clearance of HCV^{14,15} and patient response to therapy^{14,16–18}. Ensuing studies have since identified four genetic variants in linkage disequilibrium with the primary tag SNPs^{19–21}. One of these variants, rs368234815, is a dinucleotide frameshift variant that creates *IFNL4*, a gene upstream of *IFNL3* (ref. 22). Paradoxically, expression of *IFNL4* correlates with viral persistence. The mechanism behind this correlation has yet to be fully elucidated. We identified rs4803217, located in the 3' untranslated region (3' UTR) of *IFNL3*, as a functional SNP that determines HCV clearance by altering *IFNL3* expression⁴. We further showed that the protective allele (G/G, rs4803217) increases expression of *IFNL3* by escaping both AU-rich element-mediated decay and post-transcriptional regulation by HCV-induced miRNAs, miR-208b and miR-499a-5p. IFN λ 3 is a

¹Department of Immunology, University of Washington, Seattle, Washington, USA. ²Biogen-Idec Inc., Cambridge, Massachusetts, USA. ³Cancer and Inflammation Program, Laboratory of Experimental Immunology, Leidos Biomedical Research–Frederick, Frederick National Laboratory for Cancer Research, Frederick, Maryland, USA. ⁴Ragon Institute of Massachusetts General Hospital, Massachusetts Institute of Technology and Harvard University, Boston, Massachusetts, USA. ⁵Department of Medicine and Genetics Program, University of Arkansas for Medical Sciences, and The Central Arkansas Veterans Healthcare System, Little Rock, Arkansas, USA. ⁶Present addresses: Molecular and Cellular Biology Program, Department of Microbiology, University of Washington, Seattle, Washington, USA (A.P.M.); Department of Molecular Genetics and Microbiology, Center for Virology, Duke University Medical Center, Durham, North Carolina, USA (S.M.H.); Sanofi-Genzyme, Cambridge, Massachusetts, USA (D.P.B.). ⁷These authors contributed equally to this work. Correspondence should be addressed to R.S. (savanram@uw.edu).

Received 1 July; accepted 15 September; published online 14 November 2016; doi:10.1038/nm.4211

potent antiviral cytokine that induces expression of interferon-stimulated genes (ISGs). A recent study using *ex vivo* HCV-infected primary human hepatocytes demonstrated that the favorable *IFNL3* genotype correlates with high ISG expression and subsequent antiviral activity in HCV-infected and adjacent cells²³. In contrast, the magnitude of ISG expression in HCV-infected livers before IFN therapy has been shown to negatively correlate with response to pegIFN- α therapy²⁴. This disparity underlines the complexity of IFN signaling in HCV infection, as well as how much remains to be understood about the interplay between virus, host and IFN therapies.

Beyond its ability to predict natural clearance of HCV, *IFNL3* genotype is also the strongest predictor of patient response to pegIFN- α plus ribavirin therapy: patients with the unfavorable allele are less likely to respond to this therapy than those with the

favorable allele^{14,16–18}. This association between *IFNL3* genotype and response to pegIFN- α therapy suggests a possible cross-regulation of these pathways during infection, yet the mechanisms guiding this are unknown.

Factors have been identified within the type I IFN signaling pathway that correlate with the success of pegIFN- α and ribavirin therapy, among them the expression of *IFNAR1* in the liver^{25,26}. *IFNAR1* is a subunit of the type I IFN receptor composed of *IFNAR1* and *IFNAR2* chains. Studies have found that patients with high hepatic *IFNAR1* mRNA responded better to IFN therapy, whereas patients who relapsed or did not respond to IFN therapy had intermediate or low hepatic *IFNAR1* mRNA, respectively^{27–31}. Since these clinical observations, studies have demonstrated that *in vitro* HCV infection or treatment of hepatocyte cells with a HCV

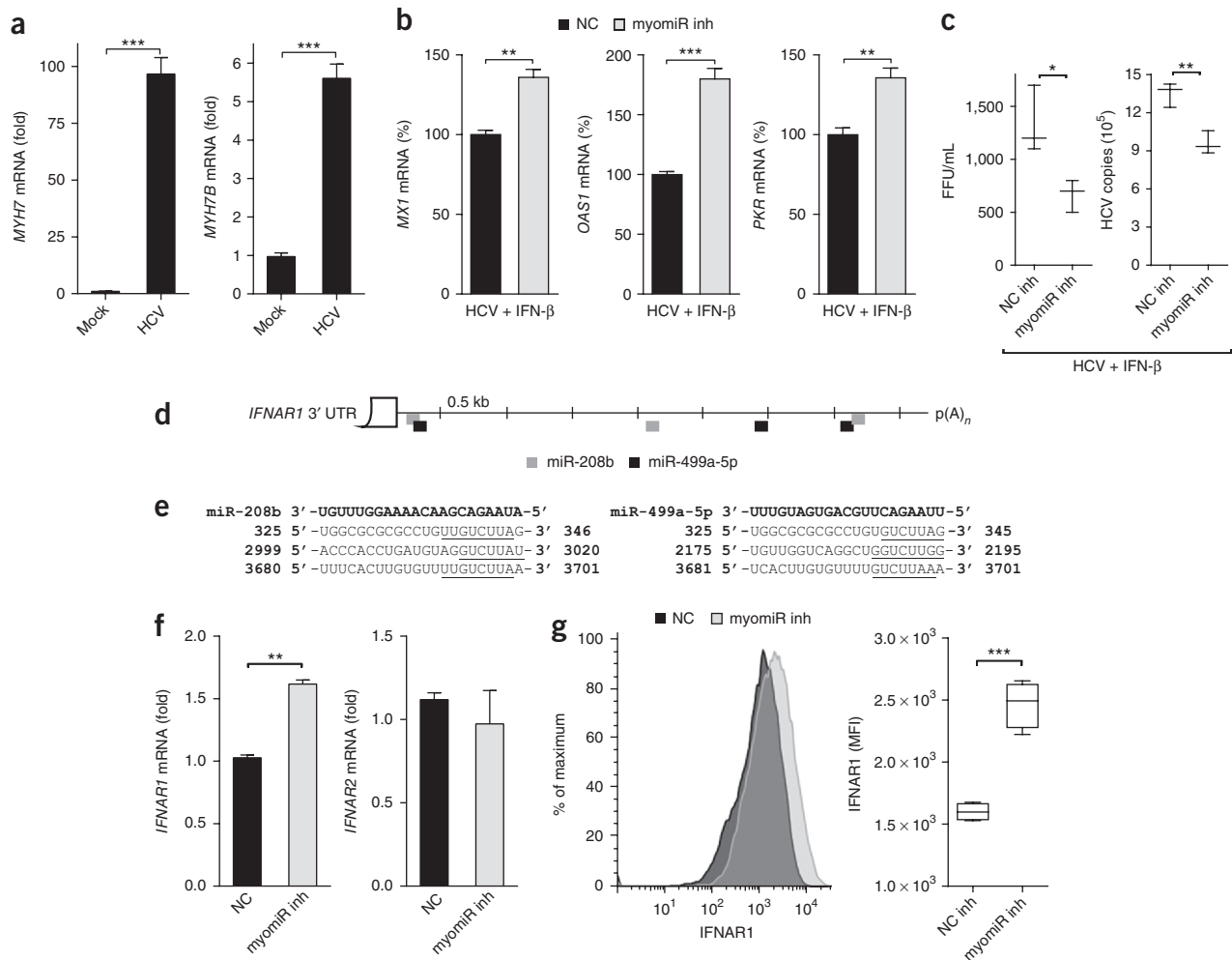


Figure 1 Inhibition of miR-208b and miR-499a-5p during HCV infection improves hepatocyte response to IFN- β by increasing IFNAR1. **(a)** Expression of *MYH7* and *MYH7B* in Huh7 cells infected with HCV MOI 1.0 for 48 h. **(b)** Expression of ISGs *MX1*, *OAS1* and *PKR* in HCV-infected Huh7 cells transfected with inhibitors against miR-208b and miR-499a-5p (myomiR inh) or non-targeting control inhibitor (NC) for 48 h and then treated with IFN- β for 6 h. **(c)** HCV viral titer and copy number from samples in **(b)**. **(d,e)** RNA hybrid analysis was used to show miRNA–target interactions for miR-208b and miR-499a-5p, which bind to numerous sites of the *IFNAR1* 3' UTR. **(d)** Schematic of miR-208b and miR-499a-5p binding sites on the *IFNAR1* 3' UTR. p(A)_n, poly(A) site. **(e)** Sequence alignment of miR-208b and miR-499a-5p and their binding sites in the *IFNAR1* 3' UTR; miRNA–target seed regions are underlined and nucleotides for *IFNAR1* 3' UTR are indicated. **(f)** Levels of *IFNAR1* and *IFNAR2* mRNA and **(g)** IFNAR1 surface protein expression in HCV-infected Huh7 cells transfected with myomiR inh or NC inh. Gene expression for **a–c,f** was assessed using qPCR, and the reference sample for relative quantification was **(a–c,f)** mock-infected cells transfected with myomiR inhibitors or NC inhibitor assayed at 48 h or **(f)** HCV-infected cells transfected with NC inhibitor assayed at 48 h. Data are from one experiment representative of three or more experiments (**a,b,f**, mean \pm s.e.m.; **c,g**, box and whisker plots show median values (line), 50th percentile values (box outline) and minimum and maximum values (whiskers)). Unpaired Student's *t*-test was used for all statistical comparisons; **P* < 0.05, ***P* < 0.01, ****P* < 0.001.

subgenomic replicon induces the unfolded protein or endoplasmic reticulum stress response in hepatoma cells that indirectly decreases *IFNAR1* protein levels^{32,33}. While these data provide insight into one mechanism regulating *IFNAR1* surface expression during HCV infection, a mechanism that explains decreased *IFNAR1* mRNA

levels in HCV infected patients has yet to be described. Moreover, no study has indicated a HCV-specific factor that directly reduces *IFNAR1* expression.

miRNAs regulate gene expression by guiding mRNA degradation machinery to complementary sequences in the 3' UTR of mRNAs³⁴.

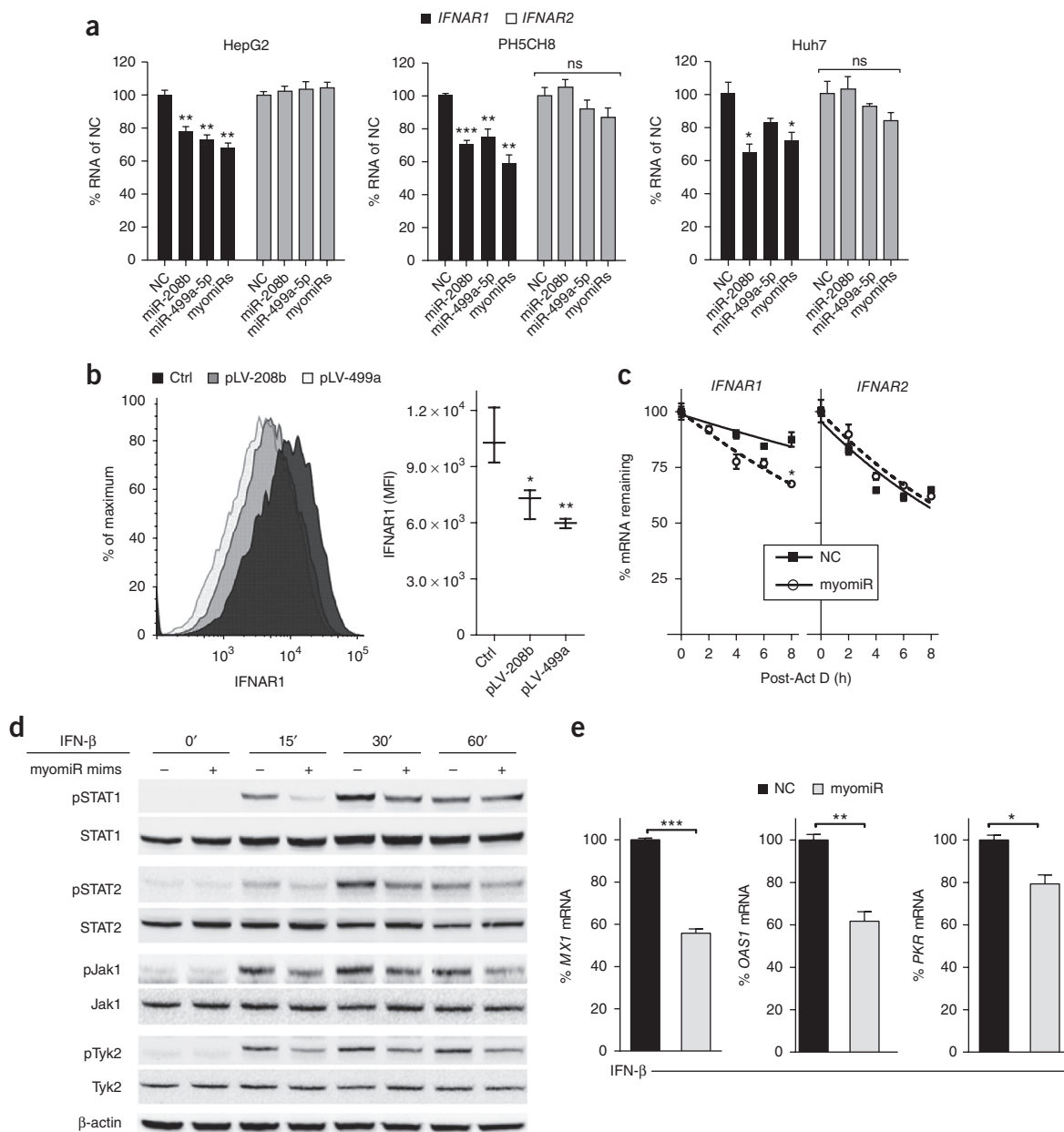


Figure 2 myomiR overexpression reduces *IFNAR1* expression, dampening downstream Jak-STAT signaling and induction of ISGs. **(a)** *IFNAR1* and *IFNAR2* mRNA expression in the hepatocyte cell lines HepG2, PH5CH8, or Huh7 transfected with mimics for miR-208b, miR-499a-5p, a mixture of both mimics (myomiRs) or a control mimic (NC). Reference sample for relative expression was NC-transfected cells. ns, non-significant. **(b)** *IFNAR1* surface protein expression in HepG2 cells stably overexpressing miR-208b (pLV-208b) or miR-499a-5p (pLV-499a-5p). **(c)** Stability of *IFNAR1* and *IFNAR2* mRNA in HepG2 cells transfected with myomiR mimics or NC mimic and treated with actinomycin D to arrest new transcription, presented as mRNA remaining over time relative to that at 0 h, set as 100%. $R^2 \geq 0.63$ for all curve fits. Half-lives (50% mRNA remaining): *IFNAR1*, 34.5 h (NC) and 14.1 h (myomiR); *IFNAR2*, 9.9 h (NC) and 10.5 h (myomiR). * $P = 0.0003$ (F test). **(d)** Immunoblot of lysates from HepG2 cells transfected with myomiR mimics or NC mimic and stimulated with 500 IU/mL IFN- β for 0, 15, 30, or 60 min. Blot was probed for STAT1, STAT2, Jak1, Tyk2 and their phosphorylated forms. β -actin was run as a loading control. **(e)** Expression of ISGs *MX1*, *OAS1* and *PKR* in HepG2 cells transfected with myomiR mimics or NC mimic stimulated with 500 IU/mL IFN- β for 6 h. Relative quantification was computed using the respective unstimulated cells then normalized to NC fold change and expressed as % mRNA of NC. Data are from **(a)** one experiment of four experiments with similar results, **(b)** one experiment representative of two experiments with four replicates per group or **(c–e)** one experiment of two experiments with similar results **(a, c, e, mean \pm s.e.m.; b, c, g, box and whisker plot shows median values (line) and minimum and maximum values (whiskers)). One-way ANOVA **(a)** or unpaired Student's t -test **(b, c, e)** was used for statistical comparison, * $P < 0.05$, ** $P < 0.01$, *** $P < 0.001$.**

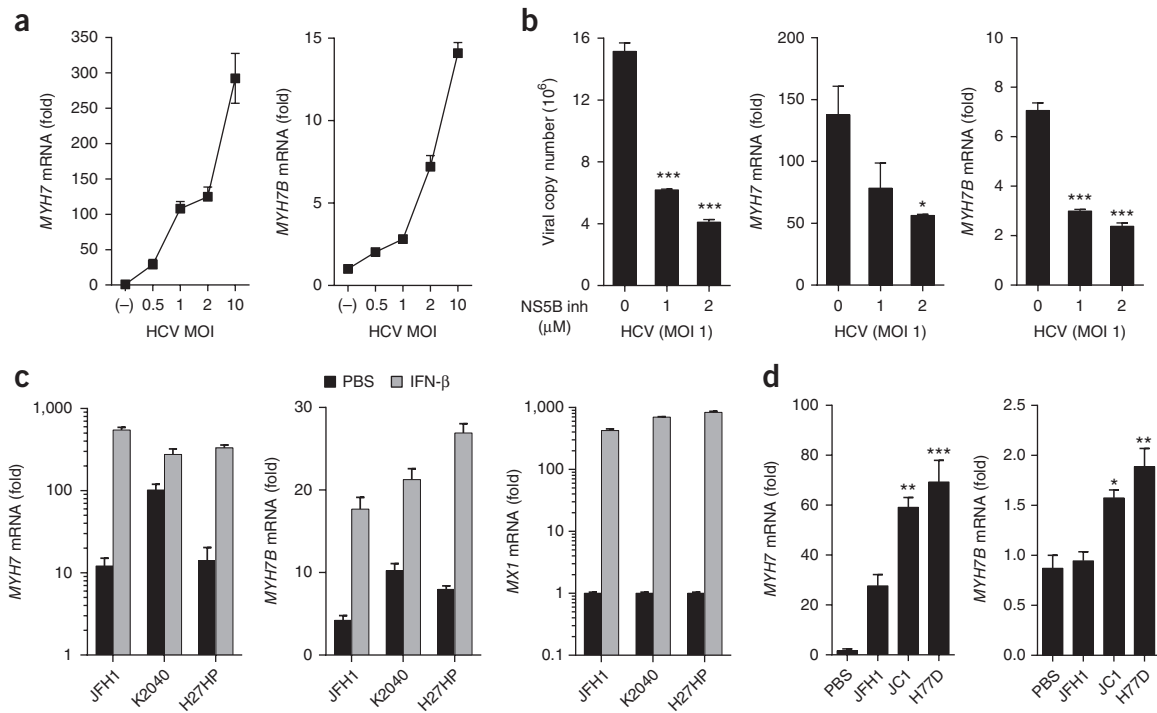


Figure 3 Myosin induction is dependent on viral replication. **(a)** Huh7 cells were infected with increasing MOIs of virus or mock-infected for 48 h and expression of *MYH7* and *MYH7B* was assessed. **(b)** Huh7 cells infected with HCV for 24 h were treated with increasing doses of NS5B inhibitor. Viral copy number, *MYH7* and *MYH7B* expression were assessed 24 h post treatment. **(c)** Huh7 cells harboring the Con1-derived bicistronic K2040 or high-passage (HP) subgenomic HCV RNA replicons (Huh7-K2040 and Huh7-HP cells respectively) or Huh7 cells harboring JFH-1-derived bicistronic HCV replicon were plated and 24 h later treated with PBS or 100 IU/mL IFN- β . 24 h later cells were lysed and expression of *MYH7*, *MYH7B* and *MX1* was measured by qPCR. **(d)** PH5CH8 cells were transfected with *in vitro* transcribed full-length HCV RNA genomes of JFH1, JC1 or H77D HCV viral strains. 48 h post transfection, cells were lysed and expression of *MYH7* and *MYH7B* was assessed by qPCR. Reference sample for relative quantification was **(a)** mock-infected cells, **(b)** untreated HCV-infected cells, **(c)** unstimulated Huh7.5 cells, or **(d)** untreated mock-transfected (PBS) PH5CH8 cells. Data are from **(a–c)** one experiment representative of two or three experiments or **(d)** four biological replicates pooled (**a–d**; mean \pm s.e.m.). One-way ANOVA (**a,d**) or unpaired Student's *t*-test (**b,c**) was used for statistical comparison. Welch's correction was applied to samples in **(c)** with unequal variance as determined by *F*-test. * $P < 0.05$, ** $P < 0.01$, *** $P < 0.001$.

We previously demonstrated that HCV infection induces expression of miR-208b and miR-499a-5p (ref. 4), two miRNAs not normally expressed in the liver. We hypothesized that within innate immune signaling pathways these miRNAs may target multiple genes in addition to *IFNL2* and *IFNL3*. miR-208b and miR-499a-5p are termed “myomiRs” as they are encoded in the introns of two myosin-encoding genes, myosin heavy chain 7 (*MYH7*) and myosin heavy chain 7B (*MYH7B*), respectively³⁵. Studies of miR-208b and miR-499a-5p in myofibers have shown that expression of these myomiRs correlates with expression of their respective parental genes *MYH7* and *MYH7B*³⁵. We found a significant correlation between transcript levels of *MYH7* and *MYH7B* with their intronic pri-miRNAs and mature miRNAs in liver biopsies from patients chronically infected with HCV. This demonstrates that *MYH7* and *MYH7B* expression can be used as a surrogate readout for myomiR expression⁴. Since HCV clearance depends on the host response to endogenous type I IFNs and/or therapeutic pegIFN- α , we were interested in determining whether these myomiRs targeted effectors in the type I IFN signaling pathway.

To investigate the effects of HCV-induced myomiRs on type I IFN signaling, we used previously characterized locked nucleic acid (LNA) inhibitors to inhibit endogenous miR-208b and miR-499a-5p during HCV infection of the hepatoma cell line Huh7 (ref. 4). A LNA inhibitor with a non-targeting sequence that does not bind to any known miRNA was used as a non-targeting control (NC). Huh7

cells were transfected with myomiR inhibitors or an NC inhibitor, infected with HCV, and then treated with IFN- β . Exogenous IFN- β was used to mimic therapeutic and paracrine type I IFN signaling, as HCV disrupts signaling downstream of the helicase RIG-I (retinoic-acid-inducible gene), an essential pathogen-recognition receptor important for IFN induction. We confirmed that miR-208b, miR-499a-5p and their parental myosin genes were induced following infection as documented in our previous study⁴ (**Fig. 1a**, **Supplementary Fig. 1a**). As expected, expression of the ISGs Mx GTPase (encoded by *MX1*), 2'-5' oligoadenylate synthetase (*OAS1*) and the translational inhibitor *PKR* were all induced following IFN- β stimulation (**Fig. 1b**). Interestingly, induction of these ISGs was significantly higher in cells treated with the myomiR inhibitors compared to the non-targeting control. Increased ISG expression in myomiR inhibitor-transfected cells correlated with decreases in viral titer and RNA copy number (**Fig. 1c**). The effect of the inhibitors was dependent on HCV infection and IFN- β treatment, as there was no difference in ISG expression in either HCV-infected cells treated with inhibitors or mock-infected cells treated with IFN- β (**Supplementary Fig. 1b,c**). In this system, type III IFNs had no measurable effect, and the difference seen in ISG expression was downstream of type I IFN in the presence of myomiRs (**Supplementary Text 1**; **Supplementary Fig. 2a–e**). Together these findings suggested that myomiR-regulated factor(s) influenced

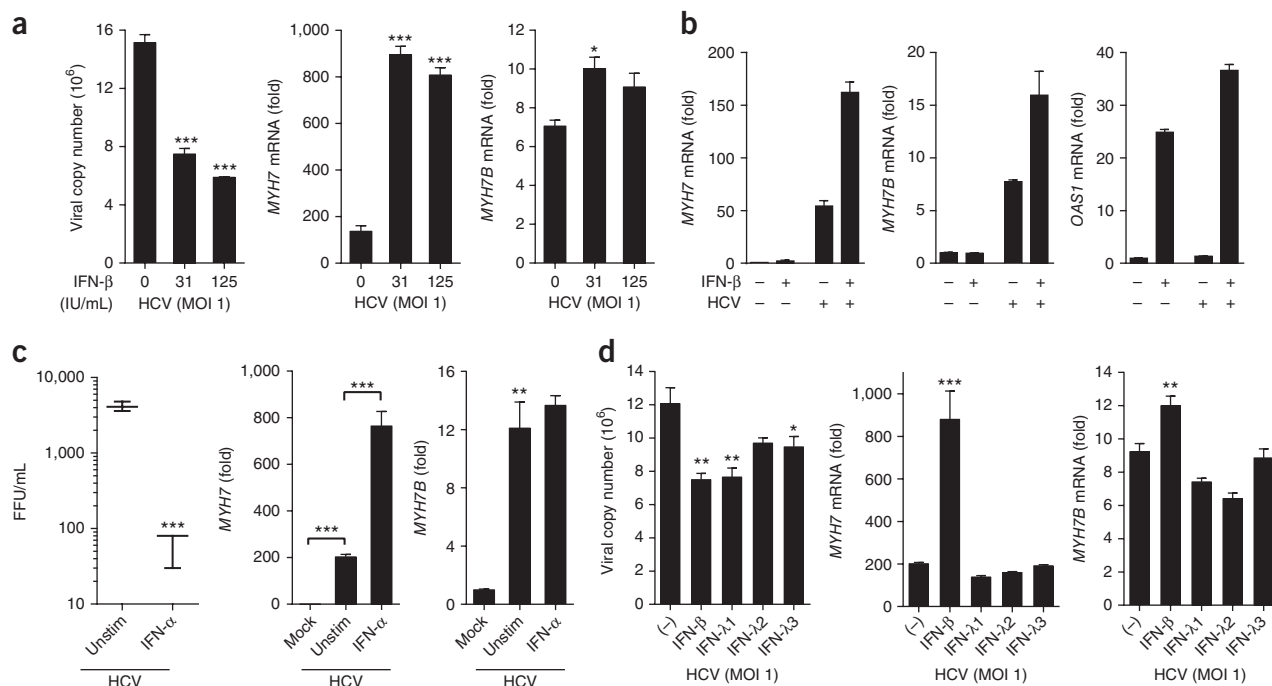


Figure 4 Type I but not type III IFNs amplify myosin expression. Huh7 cells infected with HCV MOI 1.0 for 24 h were treated with (a) increasing doses of IFN-β, (b) 31 IU/mL IFN-β, (c) 100 ng/mL of IFN-α or (d) 100 ng/mL of IFN-λ1, IFN-λ2 or IFN-λ3 or 30 IU/mL of IFN-β. 24 h post treatment, viral copy number, *MYH7*, *MYH7B* (a–c) and *OAS1* (b) expression were assessed. Reference sample for relative quantification was unstimulated HCV-infected cells. Data are from one experiment representative of two or three experiments (a–d; mean ± s.e.m., c; box and whisker plots show median values (line), 50th percentile values (box outline) and minimum/maximum values (whiskers)). Unpaired Student's *t*-test was used for all statistical comparisons, **P* < 0.05, ***P* < 0.01, ****P* < 0.001. IU, international units; FFU, focus-forming units.

hepatocyte responsiveness to IFN-β and, importantly, that myomiR inhibition improved the anti-HCV response.

As our data revealed that myomiR inhibition increased expression of multiple antiviral ISGs during HCV infection, we hypothesized that myomiRs may target an upstream effector in the type I IFN pathway. Given that reduced *IFNAR1* mRNA has been reported in HCV-infected livers^{27–31}, we investigated whether *IFNAR1* mRNA could be targeted by these myomiRs. Computational analysis revealed that the *IFNAR1* 3' UTR harbors multiple predicted miRNA recognition elements (MREs) for both miR-208b and miR-499a-5p (Fig. 1d,e). This suggests that these myomiRs may regulate *IFNAR1*. To explore this further, we transfected myomiR inhibitors or an NC inhibitor into HCV-infected Huh7 cells. We discovered that myomiR-inhibitor-transfected cells had significantly higher *IFNAR1* mRNA and cell surface expression than NC-transfected cells (Fig. 1f,g). In contrast, expression of *IFNAR2*, which does not harbor MREs for the myomiRs in its 3' UTR, was unaffected by the myomiR inhibitors (Fig. 1f). This demonstrated that the HCV-induced myomiRs, miR-208b and miR-499a-5p, specifically reduced expression of the *IFNAR1* subunit. In a pattern similar to that seen in HCV infection (Fig. 1b), cells transfected with the myomiR mimics also showed reduced pSTAT1 and ISG induction compared to control mimic-treated cells (Supplementary Text 2, Fig. 2a–e). To confirm *IFNAR1* targeting by miR-208b and miR-499a-5p, we used a firefly luciferase reporter assay where we cloned the human *IFNAR1* 3' UTR downstream of the firefly luciferase gene. We observed decreased luciferase expression when the *IFNAR1* 3' UTR luciferase construct was transfected into HepG2 cells overexpressing miR-208b or miR-499a-5p (Supplementary Fig. 1f). Taken together, these observations reveal that miR-208b and miR-499a-5p antagonized type I IFN signaling

by destabilizing and down-regulating *IFNAR1*, leading to dampened ISG expression.

As myomiRs targeted components of the type I and type III IFN pathways, which are central to the antiviral response against HCV, we reasoned that understanding myomiR induction and regulation could lead to the discovery of new antiviral targets. As there is a strong correlation between expression of miR-208b and miR-499a-5p with their parental genes, we used expression of *MYH7* and *MYH7B* as surrogate readouts for myomiR expression in the current study.

We previously showed that *MYH7* and *MYH7B* are not induced in Huh7 cells during infection with West Nile virus or Sendai virus, nor are they induced following stimulation with the HCV 3' UTR PAMP or poly(I:C)⁴. In addition, we did not observe myosin expression in Dengue virus-infected Huh7 cells (Supplementary Fig. 3b). Thus, all data to date suggest that myomiR/myosin induction is specific to HCV infection. We have also observed that *MYH7* and *MYH7B* expression in JFH1 HCV-infected Huh7 cells correlated with the multiplicity of infection (MOI) (Fig. 3a). Interestingly, treatment of HCV-infected Huh7 cells with a 2'-C-methyladenosine nucleoside analog inhibitor of HCV RNA-dependent RNA polymerase (NS5B) that blocks viral genome replication and reduces viral load^{36,37} also blocked *MYH7* and *MYH7B* induction in a dose-dependent fashion (Fig. 3b). Using the HCV replicon system, we also observed that viral replication in the absence of viral entry was sufficient to induce myosin expression (Supplementary Text 3, Fig. 3c,d). These data suggested that myosin expression was dependent on viral replication.

As type I and type III IFNs inhibit HCV replication, we reasoned that IFN treatment would also reduce myosin expression. Like NS5B inhibitor treatment, prolonged type I IFN treatment of HCV-infected Huh7 cells reduced viral titer and copy number (Fig. 4a–c;

Supplementary Fig. 3c). However, treatment with either IFN- α or IFN- β dramatically increased *MYH7* expression in HCV-infected cells compared to untreated infected cells, suggesting a role for type I IFNs in the regulation of *MYH7* (**Fig. 4a–c**). In line with this observation, type I IFN treatment of the Huh7 cell lines Huh7-K2040, Huh7-HP and Huh7-JFH1 that harbor HCV replicons also amplified *MYH7* expression (**Fig. 3c**). However, unlike type I IFNs, type III IFNs did not synergize with HCV to augment expression of myosin genes (**Supplementary Text 4, Fig. 4a–d**). These data suggest that myomiRs connect the type I and III IFN pathways during HCV infection as type I IFNs can increase myomiRs, which consequently regulate type III IFN production and type I IFN signaling (**Supplementary Text 5**).

Here we have shown that the HCV-induced myomiRs, miR-208b and miR-499a-5p, decrease IFNAR1 expression by destabilizing its mRNA transcript. miRNA repression of *IFNAR1* was sufficient to decrease IFNAR1 surface expression and dampen the antiviral response to type I IFN. During HCV infection of hepatocytes, we observed that myomiR inhibitors rescued expression of IFNAR1 and amplified the antiviral response to type I IFN, resulting in decreased viral load. Based on these data and our previous observation that inhibition of myomiRs rescues expression of *IFNL2* and the risk allele of *IFNL3* during HCV infection, myomiR inhibition could aid in a multistep fashion by increasing both hepatocyte production of type III IFNs and responsiveness to pegIFN- α . This would be particularly relevant during IFN-based therapies, considering that we found that type I IFNs increase myosin/myomiR expression (**Fig. 4**). The ability of type I IFNs to amplify myosin expression, a surrogate readout for myomiR expression, is also interesting in terms of type I IFN signaling feedback. myomiRs may function to blunt the cellular response to secondary type I IFN signaling, including the production of type III IFNs, which can be induced by prolonged type I IFN stimulation³⁸ (**Supplementary Fig. 4**).

It is remarkable that unlike treatment with type I IFNs, treatment of HCV-infected hepatocytes with type III IFNs did not induce myosin/myomiR expression, raising the possibility that type III IFN-based therapies will bypass IFN induction of these myomiRs. Currently, IFN- λ -based therapy is in phase 3 clinical trials, and results from phase 2 trials have shown it to be as effective as pegIFN- α with fewer adverse effects; this suggests that IFN- λ may be a viable replacement for pegIFN- α ^{39,40}. myomiR inhibition may also benefit patients on IFN-free DAA regimens by increasing endogenous type III IFN production and type I IFN signaling. Taking these results together with our previous finding that these myomiRs also target *IFNL2* and the risk variant of *IFNL3*, we conclude that myomiRs suppress both type I and type III IFN signaling during HCV infection. Collectively, these data add to our understanding of HCV immune evasion strategies and cross-talk between type I and type III IFN signaling pathways.

METHODS

Methods and any associated references are available in the [online version of the paper](#).

Note: Any Supplementary Information and Source Data files are available in the online version of the paper.

ACKNOWLEDGMENTS

This project was funded partly by the Department of Immunology, Royalty Research Fund, University of Washington (R.S.) and by National Institutes of Health grants AI108765 (R.S.), AI060389, AI40035 (M.G.), and CA148068 (C.H.H.). This project has been funded in whole or in part with federal funds from the Frederick National Laboratory for Cancer Research, under Contract No. HHSN261200800001E (M.C.). The content of this publication does not necessarily reflect the views or policies of the Department of Health

and Human Services, nor does mention of trade names, commercial products, or organizations imply endorsement by the US Government. This Research was supported in part by the Intramural Research Program of the NIH, Frederick National Lab, and Center for Cancer Research. We thank S. Lemon and C. Rice for generously providing the H77D and JCI viral strains, respectively; Y. Loo, S. Ozarkar and L. Kropp for experimental support; and C. Lim, A. Stone and the Gale and Savan labs for the discussions and feedback on the manuscript.

AUTHOR CONTRIBUTIONS

A.J., A.P.M., and R.S. designed the study. A.J. analyzed the data and wrote the manuscript. R.S. directed the study. A.J., A.P.M., J.S., R.C.J. and M.H. performed experiments. A.J., S.M.H., A.K. and S.B. performed infections and flow cytometry preparations. D.P.B. provided reagents and reviewed the manuscript. D.P.B. was an employee of Biogen Idec and owns company stock. C.H.H., M.C. and M.G. provided intellectual input.

COMPETING FINANCIAL INTERESTS

The authors declare competing financial interests: details are available in the [online version of the paper](#).

Reprints and permissions information is available online at <http://www.nature.com/reprints/index.html>.

1. El-Serag, H.B. Epidemiology of viral hepatitis and hepatocellular carcinoma. *Gastroenterology* **142**, 1264–1273.e1 (2012).
2. Lavanchy, D. Evolving epidemiology of hepatitis C virus. *Clin. Microbiol. Infect.* **17**, 107–115 (2011).
3. Shepard, C.W., Finelli, L. & Alter, M.J. Global epidemiology of hepatitis C virus infection. *Lancet Infect. Dis.* **5**, 558–567 (2005).
4. McFarland, A.P. *et al.* The favorable IFNL3 genotype escapes mRNA decay mediated by AU-rich elements and hepatitis C virus-induced microRNAs. *Nat. Immunol.* **15**, 72–79 (2014).
5. Liang, T.J. & Ghany, M.G. Current and future therapies for hepatitis C virus infection. *N. Engl. J. Med.* **368**, 1907–1917 (2013).
6. Manns, M.P. & von Hahn, T. Novel therapies for hepatitis C—one pill fits all? *Nat. Rev. Drug Discov.* **12**, 595–610 (2013).
7. Ghany, M.G., Nelson, D.R., Strader, D.B., Thomas, D.L. & Seeff, L.B. An update on treatment of genotype 1 chronic hepatitis C virus infection: 2011 practice guideline by the American Association for the Study of Liver Diseases. *Hepatology* **54**, 1433–1444 (2011).
8. Lawitz, E. *et al.* Sofosbuvir for previously untreated chronic hepatitis C infection. *N. Engl. J. Med.* **368**, 1878–1887 (2013).
9. Afdhal, N. *et al.* Ledipasvir and sofosbuvir for untreated HCV genotype 1 infection. *N. Engl. J. Med.* **370**, 1889–1898 (2014).
10. Pawlotsky, J.M. New hepatitis C therapies: the toolbox, strategies, and challenges. *Gastroenterology* **146**, 1176–1192 (2014).
11. Jayasekera, C.R., Barry, M., Roberts, L.R. & Nguyen, M.H. Treating hepatitis C in lower-income countries. *N. Engl. J. Med.* **370**, 1869–1871 (2014).
12. Pearlman, B.L. Protease inhibitors for the treatment of chronic hepatitis C genotype-1 infection: the new standard of care. *Lancet Infect. Dis.* **12**, 717–728 (2012).
13. Schinazi, R., Halfon, P., Marcellin, P. & Asselah, T. HCV direct-acting antiviral agents: the best interferon-free combinations. *Liver Int.* **34** (Suppl. 1), 69–78 (2014).
14. Rauch, A. *et al.* Genetic variation in IL28B is associated with chronic hepatitis C and treatment failure: a genome-wide association study. *Gastroenterology* **138**, 1338–1345, 1345.e1–1345.e7 (2010).
15. Thomas, D.L. *et al.* Genetic variation in IL28B and spontaneous clearance of hepatitis C virus. *Nature* **461**, 798–801 (2009).
16. Ge, D. *et al.* Genetic variation in IL28B predicts hepatitis C treatment-induced viral clearance. *Nature* **461**, 399–401 (2009).
17. Suppiah, V. *et al.* IL28B is associated with response to chronic hepatitis C interferon-alpha and ribavirin therapy. *Nat. Genet.* **41**, 1100–1104 (2009).
18. Tanaka, Y. *et al.* Genome-wide association of IL28B with response to pegylated interferon-alpha and ribavirin therapy for chronic hepatitis C. *Nat. Genet.* **41**, 1105–1109 (2009).
19. de Castellarnau, M. *et al.* Deciphering the interleukin 28B variants that better predict response to pegylated interferon- α and ribavirin therapy in HCV/HIV-1 coinfecting patients. *PLoS One* **7**, e31016 (2012).
20. di Iulio, J. *et al.* Estimating the net contribution of interleukin-28B variation to spontaneous hepatitis C virus clearance. *Hepatology* **53**, 1446–1454 (2011).
21. Pedergnana, V. *et al.* Analysis of IL28B variants in an Egyptian population defines the 20 kilobases minimal region involved in spontaneous clearance of hepatitis C virus. *PLoS One* **7**, e38578 (2012).
22. Prokunina-Olsson, L. *et al.* A variant upstream of IFNL3 (IL28B) creating a new interferon gene IFNL4 is associated with impaired clearance of hepatitis C virus. *Nat. Genet.* **45**, 164–171 (2013).
23. Sheahan, T. *et al.* Interferon lambda alleles predict innate antiviral immune responses and hepatitis C virus permissiveness. *Cell Host Microbe* **15**, 190–202 (2014).

24. Honda, M. *et al.* Hepatic ISG expression is associated with genetic variation in interleukin 28B and the outcome of IFN therapy for chronic hepatitis C. *Gastroenterology* **139**, 499–509 (2010).
25. He, X.S. *et al.* Global transcriptional response to interferon is a determinant of HCV treatment outcome and is modified by race. *Hepatology* **44**, 352–359 (2006).
26. Welzel, T.M. *et al.* Variants in interferon-alpha pathway genes and response to pegylated interferon-Alpha2a plus ribavirin for treatment of chronic hepatitis C virus infection in the hepatitis C antiviral long-term treatment against cirrhosis trial. *Hepatology* **49**, 1847–1858 (2009).
27. Fukuda, R. *et al.* Expression of interferon-alpha receptor mRNA in the liver in chronic liver diseases associated with hepatitis C virus: relation to effectiveness of interferon therapy. *J. Gastroenterol.* **31**, 806–811 (1996).
28. Fukuda, R. *et al.* Effectiveness of interferon-alpha therapy in chronic hepatitis C is associated with the amount of interferon-alpha receptor mRNA in the liver. *J. Hepatol.* **26**, 455–461 (1997).
29. Mathai, J. *et al.* IFN-alpha receptor mRNA expression in a United States sample with predominantly genotype 1a/1 chronic hepatitis C liver biopsies correlates with response to IFN therapy. *J. Interferon Cytokine Res.* **19**, 1011–1018 (1999).
30. Morita, K. *et al.* Expression of interferon receptor genes in the liver as a predictor of interferon response in patients with chronic hepatitis C. *J. Med. Virol.* **58**, 359–365 (1999).
31. Morita, K. *et al.* Expression of interferon receptor genes (IFNAR1 and IFNAR2 mRNA) in the liver may predict outcome after interferon therapy in patients with chronic genotype 2a or 2b hepatitis C virus infection. *J. Clin. Gastroenterol.* **26**, 135–140 (1998).
32. Liu, J. *et al.* Virus-induced unfolded protein response attenuates antiviral defenses via phosphorylation-dependent degradation of the type I interferon receptor. *Cell Host Microbe* **5**, 72–83 (2009).
33. Chandra, P.K. *et al.* HCV infection selectively impairs type I but not type III IFN signaling. *Am. J. Pathos.* **184**, 214–229 (2014).
34. Schwerk, J., Jarret, A.P., Joslyn, R.C. & Savan, R. Landscape of post-transcriptional gene regulation during hepatitis C virus infection. *Curr. Opin. Virol.* **12**, 75–84 (2015).
35. van Rooij, E. *et al.* A family of microRNAs encoded by myosin genes governs myosin expression and muscle performance. *Dev. Cell* **17**, 662–673 (2009).
36. Liu, S. *et al.* Measuring antiviral activity of benzimidazole molecules that alter IRES RNA structure with an infectious hepatitis C virus chimera expressing Renilla luciferase. *Antiviral Res.* **89**, 54–63 (2011).
37. Eldrup, A.B. *et al.* Structure-activity relationship of heterobase-modified 2'-C-methyl ribonucleosides as inhibitors of hepatitis C virus RNA replication. *J. Med. Chem.* **47**, 5284–5297 (2004).
38. Ank, N. *et al.* Lambda interferon (IFN-lambda), a type III IFN, is induced by viruses and IFNs and displays potent antiviral activity against select virus infections in vivo. *J. Virol.* **80**, 4501–4509 (2006).
39. Zeuzem, S. *et al.* Pegylated Interferon-Lambda (PEGIFN-L) shows superior viral response with improved safety and tolerability versus PEGIFN-2A in HCV patients (G1/2/3/4): Emergence phase IIB through week 12. *J. Hepatol.* **54**, S538–S539 (2011).
40. Muir, A.J. *et al.* A randomized phase 2b study of peginterferon lambda-1a for the treatment of chronic HCV infection. *J. Hepatol.* **61**, 1238–1246 (2014).

ONLINE METHODS

Cell culture conditions. HepG2 and PH5CH8 cell lines were obtained from ATCC. The identity of each hepatocyte cell line was confirmed based on their response to stimuli, and all cell lines tested negative for mycoplasma contamination. HepG2, Huh7, Huh7.5, PH5CH8 cells were cultured in complete DMEM (Sigma) media containing 10% heat-inactivated FBS (FBS; Atlanta Biologicals) and 1% penicillin-streptomycin-glutamine (Mediatech). HepG2 cells overexpressing miR-208b (pLV-miR-208b), miR-499a-5p (pLV-miR-499a-5p), or a non-targeting control miRNA were cultured in complete DMEM with 2 µg/mL puromycin dihydrochloride. Huh7-K2040, Huh7-HP and Huh7-JFH1 replicon cells were cultured in DMEM with 2 µg/mL G418, 1mM sodium pyruvate, 1× MEM NEAA, 2mM L-Glutamine, and 10% FBS (Hyclone, no heat inactivation). All cells were incubated at 37 °C in 5% CO₂.

IFNL1 knockout with CRISPR-Cas9 system. *IFNL1* guide RNA (gRNA, 5'-GCTCTCCCACCCGTAGACGG-3') was cloned downstream of the U6 promoter in the pRRL-U6-empty-gRNA-MND-Cas9-t2A-Puro vector using In-Fusion enzyme mix (Clontech). To generate knock out of *IFNL1* in Huh7, cells were transfected with either cas9 alone or *IFNL1* gRNA-Cas9 plasmids. For transfection of CRISPR-cas9 plasmids, 3 × 10⁶ cells were seeded onto a 10 cm dish the day before transfection. 10 µg of either cas9 alone or *IFNL1* gRNA-cas9 was transfected using the CaPO₄ transfection kit (Invitrogen) according to the manufacturer's instructions. 48 h post transfection, 2 µg/mL of puromycin was added to the media and cells were cultured for an additional week under selection before transduction efficiency was accessed. To confirm successful gene targeting in selected cells, genomic DNA was extracted from Huh7-wt/cas9 and Huh7-*IFNL1*^{-/-} cells (NucleoSpin Tissue; Clontech). The genomic region surrounding the *IFNL1* target site was amplified by PCR, forward 5'-GGTCCCAAAGCTAGGGAGGG-3' and reverse 5'-TTGTTGTACAGGTC CTGTTTCTTCAGG-3'. PCR products were evaluated by restriction fragment length polymorphism using the enzyme *Hyp166II*, the restriction site of which overlaps the *IFNL1* CRISPR targeting site.

RNA isolation, reverse transcription and quantification of gene expression. RNA was extracted using RNeasy Mini kit (Qiagen) or by using the TRIzol method (Qiagen). qPCR was carried out using the QuantiTect RT kit (Qiagen) according to the manufacturer's protocol. qPCR was carried out using the ViiA7 qPCR system with *TaqMan* reagents (Life Technologies). Gene expression levels were normalized to *HPRT* for all cell types.

Total RNA for miRNA analysis was extracted with miRNeasy Mini Kit (Qiagen) or by using the Trizol method. miRNA-RT was carried out using miRCURY LNA Universal RT according to the manufacturer's instructions (Exiqon), and SYBR qPCR master mix (Life Technologies) was used for quantitative PCR. Three LNA primers (Exiqon) designed to detect the most common miR-499a-5p isomiRs (miRBase) were pooled for detection. The miR-208b LNA primer was optimized by using a primer with a lower T_m. SNORD38B was used as an endogenous control.

miRNA mimic and inhibitor transfections and stimulations. miR-208b mimic, miR-499a-5p mimic, as well as a non-targeting control (NC) mimic that does not bind to any known mammalian genes, were purchased from Dharmacon. As commercially available inhibitors of miR-208b and miR-499a-5p (Dharmacon) had marginal efficacy of 40% in our systems, we developed LNA inhibitors specific for either miR-208b or miR-499a-5p. These custom LNA inhibitors showed a consistent 80% inhibition of their target miRNA⁴. A LNA inhibitor control in which the seed sequence of miR-499a-5p was mutated and predicted to bind no known human miRNA was used as a non-targeting control (NC). For transfection of mimics/inhibitors, cells were seeded at a density of 2-3 × 10⁵ cells/well of a 6-well plate, and 20-40 nM/well of mimics or inhibitors were transfected using 5-10 µl/well of DharmaFECT 4 transfection reagent (Dharmacon).

For all stimulations done on mimic- or inhibitor-transfected cells, 500 IU/mL of human IFN-β was used. For immunoblot analysis of HepG2 cells, cells were stimulated 48 h post-transfection with mimics and whole-cell extracts

were collected at 0, 15, 30, and 60 min. For ISG expression in HCV-infected Huh7 cells or mimic-transfected HepG2 cells, cells were stimulated 48 h post transfection with inhibitors/mimics and for the HCV-infected cells, 36 h post infection. IFN-α and IFN-β were purchased from PBL, and IFN-λ1, IFN-λ2 and IFN-λ3 were purchased from R&D Systems.

mRNA stability. Mimic-transfected HepG2 cells were treated with 10 µg/10⁶ cells/mL of Actinomycin D 48 h post transfection. Samples were taken at 0, 2, 4, 6 and 8 h post-treatment and processed for qPCR analysis. HepG2 cells treated with ActD did not show any overt toxicity at the specified concentration at 8 h.

Immunoblot analysis. 30-60 µg of lysates were subjected to SDS-PAGE and transferred to PVDF membranes (Thermo Scientific). The membranes were then probed using the recommended antibody dilution in 5% BSA in TBST (Tris-Buffered Saline and Tween 20) or 5% non-fat milk in TBST for phospho-STAT1 (Tyr701), STAT1, phospho-STAT2 (Tyr690), STAT2, phospho-Tyk2 (Tyr1054/1055), Tyk2, phospho-Jak1 (Tyr1022/1023), Jak1 or β-actin (13E5) (Cell Signaling). Validation of antibodies is provided on the manufacturer's website.

HCV infection. Cell culture-adapted HCV JFH1 genotype 2A strain was propagated and infectivity titrated, as previously described previously³⁹. For HCV infections, inhibitor-transfected cells were inoculated with virus at a Multiplicity of Infection (MOI) of 1.0 for 3 h and then the media was replaced. Cells were harvested using Trizol or RLT lysis buffer (Qiagen) at the indicated times. HCV RNA copy number was measured using quantitative qPCR with the *TaqMan* Fast Virus 1-step kit and primers specific for the 5' UTR (Pa03453408_s1, Life Technologies). The copy number was calculated by comparison to a standard curve of *in vitro*-transcribed full-length HCV RNA (Supplementary Fig. 1e).

HCV RNA transcription and transfections. Plasmids containing full-length cDNA sequences of JFH1, JC1 or H77D HCV viruses were linearized by restriction enzyme digest and purified. The linearized product was used for *in vitro* transcription using the T7 MEGascript kit (Life technologies). Following transcription, samples were DNase treated, unincorporated nucleotides were removed and the resulting RNA sample was run on a 1% formaldehyde gel to check for purity. For HCV RNA transfection, PH5CH8 cells were seeded at a density of 1.5 × 10⁵ cells/well in a 12 well plate. The next day 200 ng of HCV RNA was transfected per well using 1.125 µl mRNA Boost reagent (Mirus) and 2.25 µl TransIT-mRNA reagent (Mirus)⁴¹. Cells were harvested 48 h post transfection.

HCV viral titer. HCV viral titer was measured using a focus-forming unit (FFU) assay where 100 µl of cell supernatant was serially diluted 10 to 100-fold in complete DMEM and used to infect 8 × 10⁴ Huh-7.5 cells per well in 24 well plates. Cells incubated for 2 h, then supernatant was removed and cells were washed twice with PBS and supplemented with complete DMEM. 48 h post-inoculum cells were fixed with paraformaldehyde and incubated with an anti-HCV NS5A antibody, then the appropriate HRP-conjugated secondary. VECTOR VIP Peroxidase Substrate Kit (SK-4600) was used to visualize staining, and focal units were counted and expressed as FFU/mL of supernatant.

Statistical analysis. Unpaired Student's *t*-test and one-way ANOVA analyses were done using GraphPad Prism 6 Software. For samples with unequal variance, determined by *F*-test, Welch's correction was applied. Mean ± s.e.m. was used for statistical analyses of experiments with technical replicates noted in figure legends. For data using pooled biological replicates, the averages of technical replicates from each biological replicate were pooled and used for statistical analyses and described in the figure legends.

41. Gonzalez, G., Pfannes, L., Brazas, R. & Striker, R. Selection of an optimal RNA transfection reagent and comparison to electroporation for the delivery of viral RNA. *J. Virol. Methods* **145**, 14-21 (2007).